Numerical analysis of MHD double diffusive nano-fluid convection in a cavity using FEM

P. Nithish Reddy[1,*], K. Murugesan[2], V. Koushik[1]

1. *Mechanical Engineering Department, Sreenidhi Institute of Science and Technology, Hyderabad 501301, India*

2. *Mechanical & Industrial Engineering Department, Indian Institute of Technology Roorkee, Roorkee 247667, India*

dr.nithish.reddy@gmail.com

ABSTRACT. *In this paper double diffusive convection phenomenon in a cavity subjected to magnetic field is studied. Various investigations are conducted on heat and mass transfer rates in the cavity filled with water based nano fluid containing different nano particles including Ag, Cu and TiO_2. The side walls of the cavity are differentially heated and concentrated while both the top and bottom walls are kept adiabatic to heat and mass flow. Galerkin's weighted residual finite element method is used to solve the conservation equations namely vorticity transport equation, velocity Poisson equations, energy and mass balance equations. Maxwell-Garnett model is used for evaluating thermal conductivity ratio and Brinkman model is used in predicting the effective viscosity. Numerical investigations are carried out on the effect of parameters like magnetic field intensity, particle volume fraction, type of nano particles and thermal Rayleigh number on heat and mass transfer rates in the system. The effect of inclusion of nano particles at different levels of magnetic field intensities is studied and results obtained with different nano particles with variation in Hartmann number are compared. It is observed that maximum of 71% and 78% loss is observed in Nusselt and Sherwood numbers respectively with increment in Hartmann number from 0 to 100.The gain or loss in the ratio of Nusselt of nano fluid to that of base fluid tend to increase with increase in intensity of magnetic field and particle volume fraction.*

RÉSUMÉ. *Dans cet article, on étudie le phénomène de convection à double diffusion dans une cavité soumise à un champ magnétique. Diverses enquêtes sont menées sur les taux de transfert de chaleur et de masse dans la cavité remplie de nanofluides à base d'eau contenant différentes nanoparticules, notamment Ag, Cu et TiO_2. Les flancs de la cavité sont chauffées et concentrées de manière différentielle tout en maintenant les murs supérieure et inférieure adiabatique au flux thermiques et massiques. La méthode des éléments finis (MEF) pondérés résiduels de Galerkin est utilisée pour résoudre les équations de conservation, à savoir l'équation de transport du tourbillon, les équations de Poisson de vélocité, les équations de bilan de masse et d'énergie. Le modèle Maxwell-Garnett est utilisé pour évaluer le rapport de conductivité thermique tandis que le modèle Brinkman est utilisé pour prédire la viscosité effective. Des*

études numériques sont effectuées sur l'effet de paramètres tels que l'intensité du champ magnétique, la fraction volumique des particules, le type de nanoparticules et le nombre de Rayleigh thermique sur les taux de transfert de chaleur et de masse dans le système. L'effet de l'inclusion de nanoparticules à différents niveaux d'intensité de champ magnétique est étudié et les résultats obtenus avec différentes nanoparticules à variation du nombre de Hartmann sont comparés. Il s'agit d' une perte maximale de 71% et de 78% dans les nombres de Nusselt et de Sherwood, avec une augmentation du nombre de Hartmann de 0 à 100. Le profit ou la perte entre le rapport Nusselt du nano fluide et celui du fluide de base ont tendance à augmenter avec augmentation de l'intensité du champ magnétique et de la fraction volumique des particules.

KEYWORDS: *double diffusive convection, magnetic field, nano fluid, and cavity.*

MOTS-CLÉS: *convection à double diffusion, champ magnétique, nanofluide, cavité.*

DOI:10.3166/ACSM.42.589-612 © 2018 Lavoisier

1. Introduction

Study of double diffusive convection phenomenon has obtained good significance in both science and engineering due to its familiarity in many industrial practices and natural phenomenon (Chaves *et al.,* 2015; Reddy and Murugesan, 2017a). The interplay between thermo-solutal buoyancy forces become real essence of such flows and whole convective transport here depends on this. Many researchers simulated double diffusive convection in different controlled system and analyzed various aspects in it. An investigation on the effect of change in relative magnitude of thermo-solutal buoyancy forces on heat and mass transfer in a cavity model was carried out by Beghein *et al.* (1992). In this numerical experiment they reported the motion of fluid with respect to change in location of concentration source for different strength of solutal buoyancy forces. Nishimura *et al.* (1998) considered an opposing case where thermal and solutal buoyancy forces are counteracting each other in rectangular cavity model. They demonstrated oscillatory characteristics of the flow in such situation and the formation of secondary circulation cells when buoyancy ratio is in the limit 0-2. Another opposing flow condition in a square cavity system simulated by Ghernaout *et al.* (2014) revealed that solutal buoyancy forces intensifies the fluid circulation better compared to thermal buoyancy forces. Al-Amiri *et al.* (2007) explored the optimum heat and mass transfer parameter in a lid-driven cavity case, they reported the low heat and mass transfer conditions that had encountered when operated at certain level of buoyancy ratio and Richardson numbers. Chen *et al.* (2010) tested the applicability of a Lattice Boltzmann method in numerical modeling of a double diffusive convection system using modest grid resolution and has come out successful. Kumar *et al.* (2010; 2011) has shown the effect of introduction of inertial forces on double diffusive convection in square cavity model with and without a heated block inside. They gave correlations for heat and mass transfer rates and presented the contours representing the flow patterns for wide range of parameters that are considered in the study. Mahapatra *et al.* (2013) reported an exclusive study on effect of buoyancy ratio in a lid driven cavity model, they used staggered grid finite difference method in this simulations. Lee and Hyun (1997) studied double diffusive convection under horizontal temperature and concentration gradients for low, medium

and high range of buoyancy ratios. They observed an interesting multi-layered flow structures in the core of the cavity for medium range of buoyancy ratios. Qin *et al.* (2014) and Corinne *et al.* (2015) studied double diffusive convection in differentially heated and salted rectangular and square cavities respectively and gave correlations for heat and mass transfer. Naziari *et al.* (2015) investigated the effect of hot obstacle on double diffusive convection inside a square cavity, they reported that high Rayleigh number promotes multi-layered fluid structure and high buoyancy ratio vanishes vortices. Few other investigations on double diffusive convection includes Jenaa *et al.* (2015) work using non-Newtonian fluid, Reddy and Murugesan, (2017b) numerical experiments using a nano-fluid, Ren *et al.* (2016) simulations taking Soret and Doufour effect in to consideration.

Application of Magnetic field on any conducting fluid system generates Lorengz forces which can change the course of motion, in many manufacturing processes this principle is mainly used to hamper the fluid convection for better crystalline structures (Siddiqa *et al.,* 2012; Seki *et al.,* 1979; Vasanthakumari and Pondy, 2018). In fluid mechanics this kind of convection is studied under Magentohydrodynamic. Xu *et al.* (2006) experimentally demonstrated such convective motion of fluid. Following this similar investigations are documented in the literature demonstrating the response of fluid with respect to change in intensity of magnetic field (Emery, 1963; Alchaar, 2007; Reddy, 2017c). Chamka and Al-Naser (2002a, b) reported the heat and mass transfer characteristic of vertical cavity with constant temperature and flux boundary conditions under the influence of magnetic field. Teamah *et al.* (2008) in an another investigation in a vertical cavity reported that presence of heat source and heat sink could either paly positive or negative role on heat transfer for all Ha and Rayleigh numbers. Venkatachalappa *et al.* (2011) from his research on MHD double diffusive convention in an annular vertical cylindrical cavity reported that magnetic field could suppress thermo-solutal convection at low buoyancy ratio but could only suppress solutal convection at high buoyancy ratios. Ma (2009) had successfully simulated MHD double diffusive convection in a vertical cavity using lattice Bhatnagar-Gross-Krook model. From all the above studies it is commonly seen that magnetic field suppresses the fluid convection, in some instances like cooling of magnetic storage media, magnetic field sensors, small and large scale machineries under electromagnetic fieldsetc where the efficiency of cooling systems decreases due to presence of magnetic fields (kefayati, 2016) under such conditions it is favorable to use nano particles in working fluids to enhance the efficiency of the system. Few researchers investigated the influence of nanoparticles, Ghasemi *et al.* (2011) studied natural convection in a differentially heated square cavity under the influence of magnetic field. Here in this study they stated that increase in volume fraction may either enhance or hamper heat transfer depending upon operating Rayleigh number and Hartmann number. Mahmoudi *et al.* (2105; 2014) observed that nano particles reduces entropy generation, in this cavity flow problem they reported that effect of nano particles on heat transfer enhancement is high at higher Hartmann number. Kefayati (2013) investigated the effect of magnetic field on natural convection in an open cavity using nano fluids. Results shown that influence of particle volume fraction on heat transfer is felt more at higher Hartmann number. Ashorynejad *et al.* (2013) studied a natural convection flow of nano fluid inside a horizontal cylindrical annulus

exposed to magnetic field. They observed that radial magnetic field can effectively suppress the flow oscillations while nano particles enhance the Nusselt number. Sourtiji *et al.* (2014) in his study on MHD natural convection in a cylindrical-triangular annulus observed that Nusselt number is an increasing function of volume fraction and aspect ratio. Influence of nano particles on heat transfer augmentation is observed more at higher Hartmann number and lower Rayleigh number. Bourantas and Loukopoulos (2014) supported the above argument that both strength and orientation of magnetic field significantly affect the fluid flow and heat transfer patterns. Selimefendigil and Oztop (2014) studied MHD convection in a lid driven cavity problem with rotating cylinder inside, they observed that heat transfer enhancement is superior at higher Richardson number. They also reported that higher heat transfer rates are recorded with cylinder rotation than with motion less case.

In the literature the influence of nano particles under the influence of both heat and mass transfer subjected to magnetic field is not addressed to the best of our knowledge although decent work is available on simple natural convection cases. However such studies are useful in many applications where nano fluids are used to counteract the convective heat losses induced by magnetic fields. In the current investigation double diffusive natural convection of nano fluids under magnetic field in square cavity model with different presentation like effect of particle volume fraction, magnetic field intensity, operating Rayleigh number and type of nano particle in use are covered. Results are presented systematically using comparison of various contours and Nuseelt, Sherwood number plots for range of parameters considered.

2. Governing equations

Flow is assumed incompressible and Boussinesq approx-imation is introduced for density variation. The governing equations in velocity vorticity form are obtained as follows:

X-Momentum equation with Boussinesq approximation can be given as

$$\frac{\partial u}{\partial t}+u\frac{\partial u}{\partial x}+v\frac{\partial v}{\partial y}=-\frac{1}{\rho_{nf}}\frac{\partial P}{\partial x}+\frac{\mu_{nf}}{\rho_{nf}}\left[\frac{\partial^2 u}{\partial x^2}+\frac{\partial^2 u}{\partial y^2}\right] \tag{1a}$$

Y-Momentum equation with Boussinesq approximation can be given as

$$\frac{\partial v}{\partial t}+u\frac{\partial v}{\partial x}+v\frac{\partial v}{\partial y}=-\frac{1}{\rho_{nf}}\frac{\partial P}{\partial y}+\frac{\mu_{nf}}{\rho_{nf}}\left[\frac{\partial^2 v}{\partial x^2}+\frac{\partial^2 v}{\partial y^2}\right]+g\beta_{Tnf}\left(T-T_C\right)+g\beta_{Cnf}\left(C-C_C\right)-\sigma_{nf}B^2\frac{v}{\rho_{nf}} \tag{1b}$$

Writing momentum equation in vector form:

$$\frac{\partial V}{\partial t}+\left(V\cdot\nabla\right)V=-\frac{1}{\rho_{nf}}\nabla P+\nu_{nf}\left(\nabla^2 V\right)+F_b+F_M \tag{2}$$

where $\beta T_{nf} = -\frac{1}{\rho}\frac{\partial \rho}{\partial T}\Big|_{p,C}$ and $\beta C_{nf} = -\frac{1}{\rho}\frac{\partial \rho}{\partial C}\Big|_{p,T}$ are the thermal and solutal volumetric expansion coefficients respectively. F_b, F_M are buoyancy force and magnetic force respectively.

For converting above momentum equation in to velocity vorticity form we take curl on both sides of Eq. (2).

$$\frac{\partial \omega}{\partial t} + \nabla \times (V.\nabla V) = -\nabla \times \nabla \frac{P}{\rho_{nf}} + \nu_{nf} \nabla^2 (\nabla \times V) + \nabla \times F_b + \nabla \times F_M \tag{3}$$

Since $\nabla \times \nabla \frac{p}{\rho} = 0$, the above equation can be rewritten without the pressure term as

$$\frac{\partial \omega}{\partial t} + \nabla \times (V.\nabla V) = \nu_{nf} \nabla^2 (\nabla \times V) + \frac{\partial}{\partial x}\left[g\beta_{T_{nf}} (T - T_\infty) \right] + \frac{\partial}{\partial x}\left[g\beta_{C_{nf}} (C - C_\infty) \right] - \frac{\partial}{\partial x} \sigma_{nf} B^2 \frac{\nu}{\rho_{nf}} \tag{4}$$

Simplifying the above equation using vector relations as follows

$$(\mathrm{u} \cdot \nabla)\, \mathrm{u} = \frac{1}{2} \nabla\, (\mathrm{u} \cdot \mathrm{u}) - \mathrm{u} \times (\nabla \times \mathrm{u}) = \nabla \frac{\mathrm{u}^2}{2} - (\mathrm{u} \times \boldsymbol{\omega})$$

Taking curl of the above equation

$$\nabla \times (\mathbf{u} \cdot \nabla)\, \mathbf{u} = \nabla \times \left[\nabla \frac{\mathbf{u}^2}{2} - (\mathbf{u} \times \boldsymbol{\omega}) \right] = \nabla \times \nabla \frac{\mathbf{u}^2}{2} - \nabla \times (\mathbf{u} \times \boldsymbol{\omega}) = \nabla \times (\boldsymbol{\omega} \times \mathbf{u})$$

Since $\nabla \times \nabla \frac{\boldsymbol{u}^2}{2} = 0$, left hand side of above equation can be written using vector calculus as

$$\nabla \times (\omega \times \mathrm{u}) = (\mathrm{u} \cdot \nabla)\omega - (\omega \cdot \nabla)\mathrm{u} + \omega(\nabla \cdot \mathrm{u}) - \mathrm{u}(\nabla \cdot \omega) \tag{5}$$

$\nabla \cdot \boldsymbol{u} = 0$ (Incompressibility constraint) and $\nabla \cdot \boldsymbol{\omega} = 0$ (solenoidal vector field), equation (5) becomes

$$\nabla \times (\omega \times \mathrm{u}) = (\mathrm{u} \cdot \nabla)\omega - (\omega \cdot \nabla)\mathrm{u} \tag{6}$$

By substituting equation (6) for the second term in the equation (4), we get

$$\frac{\partial \boldsymbol{\omega}}{\partial t} + (\mathbf{u} \cdot \nabla)\ \boldsymbol{\omega} - (\boldsymbol{\omega} \cdot \nabla)\, \mathbf{u} = \upsilon_{nf} \nabla^2 \boldsymbol{\omega} + \frac{\partial}{\partial x}\left[g\beta_{T_{nf}} (T - T_\infty) \right]$$

$$+\frac{\partial}{\partial x}\left[g\beta_{C_{nf}}\left(C-C_{\infty}\right)\right]-\frac{\partial}{\partial x}\sigma_{nf}B^{2}\frac{\nu}{\rho_{nf}} \tag{7}$$

The term $(\boldsymbol{\omega}\cdot\nabla)\boldsymbol{u}$ in the above equation, by vector and tensor multiplication becomes equal to $(\nabla\boldsymbol{u})\cdot\boldsymbol{\omega}$

This term attributes to aspect of stretching and turning which is completely absent in 2D flow. Finally the equation (7) for 2D domain can be written as

$$\frac{\partial\omega}{\partial t}+\left(\mathrm{u}\cdot\nabla\right)\ \omega=\vartheta_{nf}\nabla^{2}\omega+\nabla\times F_{b}+\nabla\times F_{M}$$

$$\frac{\partial\omega}{\partial t}+\left(V\cdot\nabla\right)\omega=\vartheta_{nf}\nabla^{2}\omega+\frac{\partial}{\partial x}\left[g\beta_{T_{nf}}\left(T-T_{\infty}\right)\right]+\frac{\partial}{\partial x}\left[g\beta_{C_{nf}}\left(C-C_{\infty}\right)\right]-\frac{\partial}{\partial x}\sigma_{nf}B^{2}\frac{\nu}{\rho_{nf}} \tag{8}$$

Where V=(u, v) are the velocity components in x- and y-directions, respectively, ω is the vorticity component, T is dimensional temperature, C is dimensional concentration, σ is electrical conductivity, B is magnetic flux density.

To solve for flow field long with the above velocity vorticity equation continuity also has to be imposed, to do that we obtain another set of equations namely velocity Poisson equation.

Velocity poison equation

$$\nabla^{2}V=-\nabla\times\omega \tag{9}$$

For conservation of energy and solute concentration below equations are considered

Energy equation:

$$\frac{\partial T}{\partial t}+V.\left(\nabla T\right)=\alpha_{nf}\nabla^{2}T \tag{10}$$

Solutal concentration equation:

$$\frac{\partial C}{\partial t}+V.\left(\nabla C\right)=D_{nf}\nabla^{2}C \tag{11}$$

The non-dimensional form of equations can be achieved by substituting the following scaling parameters ς =ωL2/αf, time, τ=tαf/H2, non-dimensional temperature, θ =T−Tc/Th−Tc, non-dimensional concentration ϕ =C−Cc/Ch−Cc, X=x/H Y=y/H, U=uL/αf, V=vL/αf in the equation (8)-(11).

Finally

Non –dimensional form of vorticity transport equation:

$$\frac{\partial \varsigma}{\partial \tau}+U\frac{\partial \varsigma}{\partial X}+V\frac{\partial \varsigma}{\partial Y}=\frac{1}{\left(\left(1-\chi\right)+\frac{\chi\rho_p}{\rho_f}\right)\left(1-\chi\right)^{2.5}}Pr\left[\frac{\partial^2\varsigma}{\partial X^2}+\frac{\partial^2\varsigma}{\partial Y^2}\right]$$

$$+Ra\,Pr\left[\frac{\left(1-\chi\right)\rho_f+\frac{\chi\rho_p\beta_{T_p}}{\beta_{T_f}}}{\left(1-\chi\right)\rho_f+\chi\rho_p}\right]\frac{\partial}{\partial X}\left(\theta+N\phi\right)-\frac{\frac{\sigma_{nf}}{\sigma_f}}{\left(\left(1-\chi\right)+\frac{\chi\rho_p}{\rho_f}\right)}Ha^2\,Pr\frac{\partial V}{\partial X} \qquad (12)$$

Non –dimensional form of velocity Poisson equations

$$\frac{\partial^2 U}{\partial X^2}+\frac{\partial^2 U}{\partial X^2}=-\frac{\partial \varsigma}{\partial Y}$$
$$\frac{\partial^2 V}{\partial X^2}+\frac{\partial^2 V}{\partial X^2}=\frac{\partial \varsigma}{\partial X} \qquad (13\text{ a-b})$$

Non –dimensional form of energy equation

$$\frac{\partial \theta}{\partial \tau}+U\frac{\partial \theta}{\partial X}+V\frac{\partial \theta}{\partial Y}=\frac{K_{nf}}{K_f}\frac{\left(\rho C_P\right)_f}{\left(\rho C_P\right)_f\left(1-\chi\right)+\left(\rho C_P\right)_p\lambda}\left[\frac{\partial^2\theta}{\partial X^2}+\frac{\partial^2\theta}{\partial Y^2}\right] \qquad (14)$$

Non –dimensional form of solutal concentration equation

$$\frac{\partial \phi}{\partial \tau}+U\frac{\partial \phi}{\partial X}+V\frac{\partial \phi}{\partial Y}=\frac{1}{Le}\frac{D_{nf}}{D_f}\left[\frac{\partial^2\phi}{\partial X^2}+\frac{\partial^2\phi}{\partial Y^2}\right] \qquad (15)$$

Where non-dimensional numbers are defined as, Rayleigh number Ra= $\frac{g\beta_{T_f}\Delta T}{\alpha\nu_f}$

buoyancy ratio N= $\frac{\beta_{C_{nf}}\Delta C}{\beta_{T_{nf}}\Delta T}$, Ha=BL$\sqrt{\frac{\sigma}{\mu}}$,Prandtl number, Pr=ϑ_f/α_f and Le=ϑ_f/D_f

The effective thermal conductivity of the nanofluid is approximated by the Maxwell-Garnetts model [1; 19; 2]:

$$\frac{k_{nf}}{k_f}=\frac{k_p+2k_f-2\chi\left(k_f-k_p\right)}{k_p+2k_f+\chi\left(k_f-k_p\right)} \qquad (16)$$

Thermal diffusivity of nano fluid is given by

$$\alpha_{nf} = \frac{k_{nf}}{\left(\rho C_p\right)_{nf}} \tag{17}$$

Electrical conductivity (σ_{nf}) of the nanofluid are defined as [43]

$$\frac{\sigma_{nf}}{\sigma_f} = 1 + \frac{3\left(\frac{\sigma_s}{\sigma_f} - 1\right)\chi}{\left(\frac{\sigma_s}{\sigma_f} + 2\right) - \left(\frac{\sigma_s}{\sigma_f} - 1\right)\chi} \tag{18}$$

Effective properties of nano fluid are calculated using the following relations (Motevasel *et al.* 2017):

Heat capacitance:

$$\left(\rho C_p\right)_{nf} = (1-\chi)\left(\rho C_p\right)_f + \chi\left(\rho C_p\right)_p \tag{19}$$

Volumetric coefficient of thermal expansion:

$$\left(\rho\beta_T\right)_{nf} = (1-\chi)\left(\rho\beta_T\right)_f + \chi\left(\rho\beta_T\right)_p \tag{20}$$

Thermophysical properties of base fluid and nano particles are shown in Table 1 and effective properties are computed as shown in Table 2.

Table 1. Thermophysical properties of base fluid and nano particles

Properties	Water	Cu	TiO2	Ag
Cp(J/kg K)	4179	385	6862	235
ρ(kg/m3)	997.1	8933	4250	10500
k(W/mK)	0.613	400	8.95	429
β_T(1/K)	21e-05	1.67e-05	0.8e-05	1.8e-05
σ(S/m)	0.05	5.96E7	1.0e-10	6.3E7

Table 2. Effective properties of nano fluid

Dynamic viscosity (Brinkman 1952)	$\mu_{nf} = \mu_f \frac{1}{(1-\chi)^{2.5}}$
Density (Drew 1999)	$\rho_{nf} = (1-\chi)\rho_f + \chi\rho_p$
Mass diffusivity (Singh *et al.* 2015)	$D_{nf} = (1-\chi)D_f$
Kinematic viscosity	$\vartheta_{nf} = \frac{\mu_{nf}}{\rho_{nf}}$

Boundary conditions:

top wall:

$$U = 1, V = 0, \frac{\partial \theta}{\partial Y} = 0, \frac{\partial \phi}{\partial Y} = 0, \varsigma = \nabla \times V \tag{21a}$$

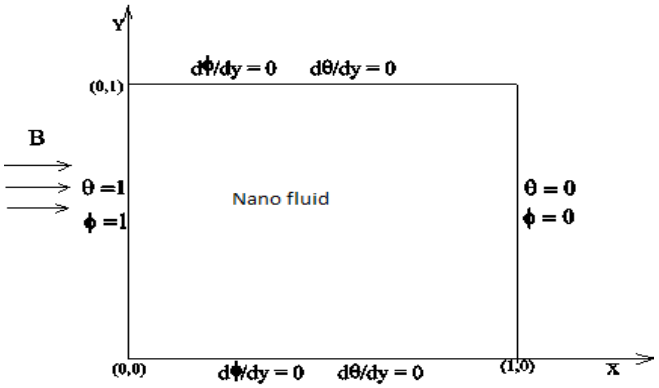

Figure 1. Schematic diagram

bottom wall:

$$U = V = 0, \frac{\partial \theta}{\partial Y} = 0, \frac{\partial \phi}{\partial Y} = 0, \varsigma = \nabla \times V \tag{21b}$$

left wall:

$$U = V = 0, \phi = 1, \theta = 1, \varsigma = \nabla \times V \tag{21c}$$

right wall:

$$U = V = 0, \phi = 0, \theta = 0, \varsigma = \nabla \times V \tag{21d}$$

Finally, the average Nusselt number and average Sherwood number are given as follows:

$$Nu = -\frac{1}{L}\int_0^L \frac{k_{nf}}{k_f}\left(\frac{\partial \theta}{\partial X}\right) dY \tag{22}$$

$$Sh = -\frac{1}{L}\int_0^L \left(\frac{\partial \phi}{\partial X}\right) dY \tag{23}$$

3. Solution methodology

Final governing equations (12-15) are solved along with the initial and boundary conditions mention above using Galerkin's' weighted residual finite element solution procedure. The obtained governing equations in integral form are solved over each element of discretized computational domain, here Transfinite interpolation (TFI) mesh generation technique is used to obtain number of bi-linear quadrilateral elements. An Isoparametric formulation is used to transform the global coordinates into local coordinate system and the Gaussian quadrature is employed for the numerical integration of all the terms in the weighted governing equations. Second order accurate Crank-Nicolson Scheme is used in discretization of time. Solutions of simultaneous non –linear equations are obtained by iteration procedure following conjugate gradient method. An in-house computer code is developed, the solution is assumed to be converged at current time step 'n+1' if the error between two successive iterations 'i' and 'i+1' for all field variables simultaneous satisfies the following relation.

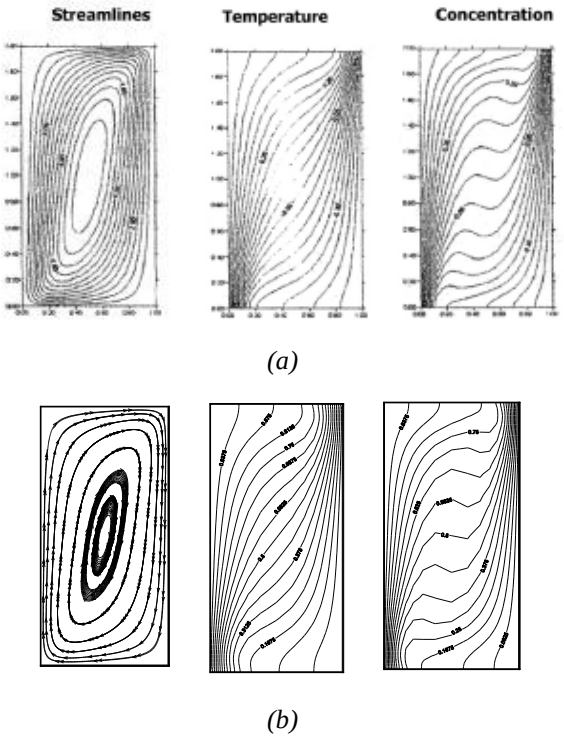

Figure 2. Comparison of stream line, temperature and concentration plots at Ra=1.0e5, Ha=25, Pr=1, Le=2 (a) Chamkha et al. (2002) (b) Present

$$\sum_{j}^{nnode}\left(\frac{\left|\left|\eta_j^{i+1}\right|-\left|\eta_j^{i}\right|\right|}{nnode}\right)\leq 10^{-5}$$

Here 'η' can be any field variable.

After the solution is obtained at current time level solution iteration procedure is repeated for next time level.

4. Results and discussion

4.1 Computational domain and validation results

Figure 1 shows the schematic diagram of computational domain subjected to magnetic field. Here vertical walls are differentially heated and slated while horizontal walls are considered adiabatic to heat and mass flow. No slip condition has been chosen for velocity over all the walls. Mesh sensitivity study has been carried out initially for three different grid sizes and a grid of 51×51 is selected for the current investigations.

The results obtained using the current code is compared for the accuracy both qualitatively and quantitatively as shown in Figures 2 and 3. Figure 2 gives the comparison of stream lines, temperature, and concentration while Figure 3 gives the comparison of Nusselt and Sherwood numbers with results that of the literature (Chamkha and Al-Naser, 2002; Teamah, 2008). Current results obtained using FEM code are found in well agreement with other literature results, hereafter this code is used for further investigations

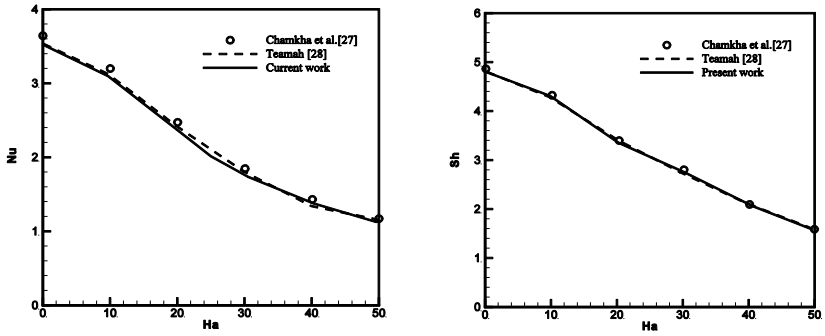

(a) *(b)*

Figure 3. Comparison of present (a) average Nusselt number and (b)Sherwood number with that of literature (Chamkha et al., 2002; Teamah, 2008) for different Hartmann numbers

4.2 Simulation results and analysis

Numerical analysis has been performed on the effect of nano particles on heat and mass transfer in square cavity under the influence of magnetic field. Results are reported for variation in flow, energy and concentration fields at different operating Rayleigh number, particle volume fraction, particle type and magnetic field intensity. Buoyancy ratio and Prandtl number are fixed at -0.75 and 7 respectively, Lewis number is taken as 2.0 for the present work.

Figure 4 presents the variation in stream lines, iso-therms, iso-concentration plots with respect to change in Hartmann number at Rayleigh number equal to 1.0e6. The dotted lines in these contours correspond to results obtained without nano particles and the solid lines give the results corresponding to cu-water nano fluid with particle volume fraction equal to 0.05. Figure 4 shows that with increase in Hartmann number the fluid circulation pattern changes and the addition of nano particles slightly alters the fluid motion

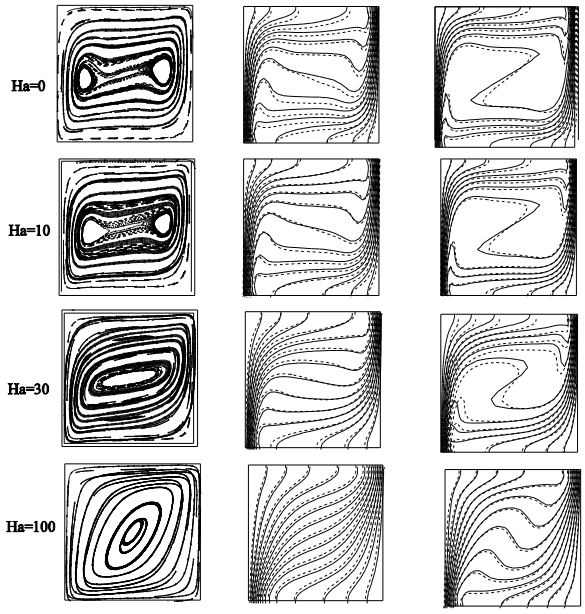

Figure 4. Effect of Hartmann number on (a) stream lines, (b) temperature (c) concentration fields when operating Rayleigh number = 1.0e6, particle volume fraction =0.0 (doted lines), 0.05 (solid lines)

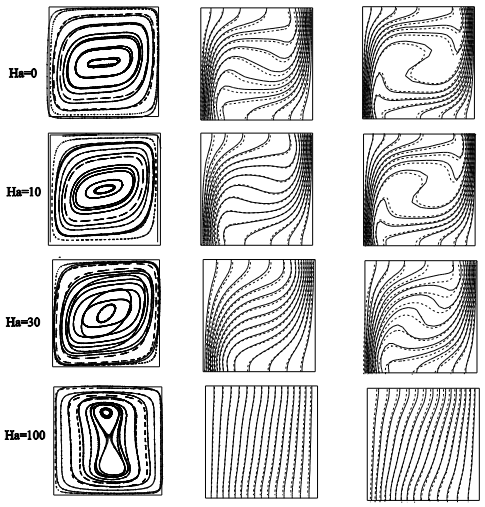

Figure 5. Effect of Hartmann number on (a) stream lines, (b) temperature (c) concentration fields when operating Rayleigh number = 1.0e5, particle volume fraction =0.0 (doted lines), 0.05(solid lines)

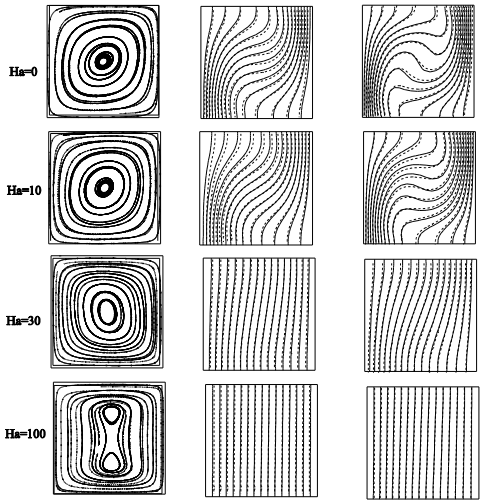

Figure 6. Effect of Hartmann number on (a) stream lines, (b) temperature (c) concentration fields when operating Rayleigh number = 1.0e4, particle volume fraction =0.0 (doted lines), 0.05(solid lines)

Isotherms and Iso-concentration lines here indicates that when the fluid is subjected to increasing magnetic intensity the heat and mass transfer rates decreases, from the figure it can be seen that the isotherms and Iso-concentration lines found less curvier at Ha=100. This can be due to loss in convective transport of heat and mass. In case of Ra=1.0e5(see Figure 5) at Ha=100 these lines turned lot straighter, this clearly suggests that magnetic field hampers the convective heat and mass transport process. Similarly when operating Rayleigh number equal to 1.0e4(see Figure 6) such phenomenon is repeated at Ha=100, another important observation is that a vertical dumble like structure is formed when magnetic intensity is high i.e at Ha=100 for all three Rayleigh number, this vertical elongation may be due to influence of magnetic forces on flow components. Because the magnetic field is acting in horizontal direction, the line of action of Lorentz force will be along the vertical axis. Hence here the flow components in vertical directions are influenced more than horizontal components.

Table 3. Average Nusselt number for different Ra and Ha values when particle volume fraction is zero

Nu	Ha=0	Ha=10	Ha=30	Ha=100	%Loss
Ra=1e4	1.93	1.601	1.170	1.157	40.082
Ra=1e5	4.05	3.717	2.443	1.176	70.991
Ra=1e6	8.08	7.788	6.300	2.785	65.557

Table 4. Average Sherwood number for different Ra and Ha values when particle volume fraction is zero

Sh	Ha=0	Ha=10	Ha=30	Ha=100	%Loss
Ra=1e4	2.41	2.066	1.082	1.073	55.51
Ra=1e5	4.92	4.561	3.231	1.099	77.68
Ra=1e6	9.96	9.61	7.916	3.858	61.28

Table 3 and 4 gives the average Nusselt number and Sherwood number respectively recorded a different Hartmann and Rayleigh numbers when no nano particles are added. These results show that Nusselt number and Sherwood number decreases with increase in Hartmann number at all three Rayleigh numbers. At Ha=100 least Nusselt and Sherwood numbers are recorded, the degree of decrement in Nusselt and Sherwood number with increase in value of Ha from 0 to 100 is displayed in the last column of the tables. The percentage loss in Nusselt and Sherwood number are found high when the operating Rayleigh number is 1.0e5 and low when the operating Rayleigh number is 1.0e4. The results corresponding to the effect of addition of nano particles are reported in figures 7 and 8, here Nu^*, Sh^*

indicates the ratio of Nusselt number or Sherwood number with nano particles to that of without nano particles

Figure 7 shows the influence of nano particles on heat transfer rates with respect to change in intensity of magnetic field at different operating Rayleigh numbers. At Ra=1.0e4 (see Figure 7a), the effective Nusselt number dominated for higher Hartmann number case and almost no difference is observed in results for Ha=30 and 100. Since effective Nusselt number (Nu*) gives the compassion of actual Nusselt number at given particle volume fraction to that of without nano-particles, at VF=0 its value is unity. Here increase in Hartmann number results in hampering of fluid convection and the results reveals that increment in Nu* with addition of nano particles is higher at stronger intensity of magnetic field. At Ha =30 here the fluid had already reached static state and thus any increment in Ha beyond 30 has not influenced Nu*.

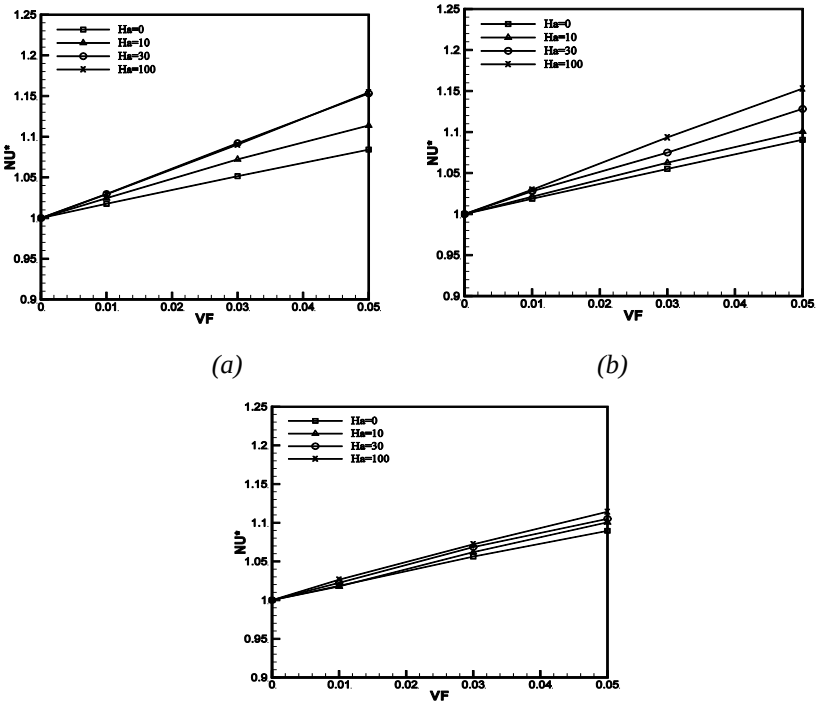

(a) *(b)*

(c)

Figure 7. Effect of particle volume fraction on effective Nusselt number at different Hartmann numbers for operating Rayleigh numbers (a) Ra=1.0e4 (b) Ra=1.0e5 and (c) Ra=1.0e6

At Ha=0 where no magnetic field is acting, the fluid circulation is not interrupted and the increment in Nu* is observed to be low. This shows that increment in Nu* is

observed more when heat transfer is in conduction mode than that of convective mode. Here Nu* is always positive, this shows that addition of nano particles augments heat transfer rates either with or without the magnetic field. At Ra=1.0e5 (see Figure 7b) fluid convection is stronger and the heat transfer had become diffusion dominant only at Ha=100 unlike at Ha=30 in previous case. Here too the increment in intensity of magnetic field yielded better results, the relative advantage of addition of nano particle is observed more at higher Hartmann number. The slopes of the lines in the plot indicates that the increment in Nu* by addition of nano particles is observed slightly more at Ra=1.0e4 compared to Ra=1.0e5 and relatively less at Ra=1.0e6. As the convection strength is strong at higher Rayleigh number (Ra=1.0e6), higher intensity of magnetic field is required to bring the fluid to rest. Therefore even at Ha=100 heat transfer occurred in convection mode unlike at Ra=1.0e4 and Ra=1.0e5 where it was conduction dominant. Also the Nusselt number lines are observed relatively closer at Ra=1.0e6 (see Figure 7c) indicating the relative effect of change in magnetic intensity on the flow field is low due to strong buoyancy induced circulation.

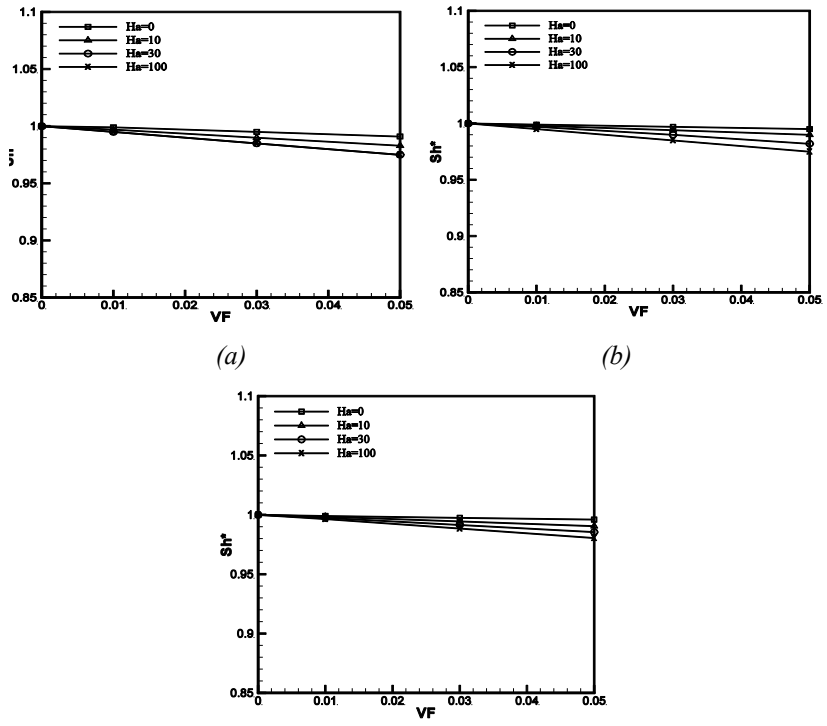

Figure 8. Effect of particle volume fraction on effective Sherwood number at different Hartmann numbers for operating Rayleigh numbers (a) Ra=1.0e4 (b) Ra=1.0e5 and (c) Ra=1.0e6

Similarly figure 8 gives the comparison of effective Sherwood number (Sh*) with respect change in particle volume fraction at different levels of magnetic field intensities. Figure 8a gives the results corresponding to operating Rayleigh number Ra=1.0e4. Firstly at Ha=0 i.e in absence of magnetic field upon addition of nano particles, the enhanced thermal characteristics of nano fluid has shown lesser control over the mass transfer of the system. Here Sherwood number (Sh*) slightly decreased with inclusion of nano particles and in presence of magnetic field such reduction is observed more. Figure 8a gives the comparison at Ra=1.0e4, here it is seen that Sh* is recorded low at higher Hartmann number indicating that suppression of fluid convection shows negative effect. At higher Rayleigh number (See Figure 8b, 8c) where fluid convection is stronger the reduction in Sh* with addition of nano particles is found slightly low compared to Ra=1.0e4. Here hampering of fluid convection with application of magnetic field resulted in fall of Sh*. This shows the relative loss in mass transfer with inclusion of nano particles is more when the fluid circulation is low.

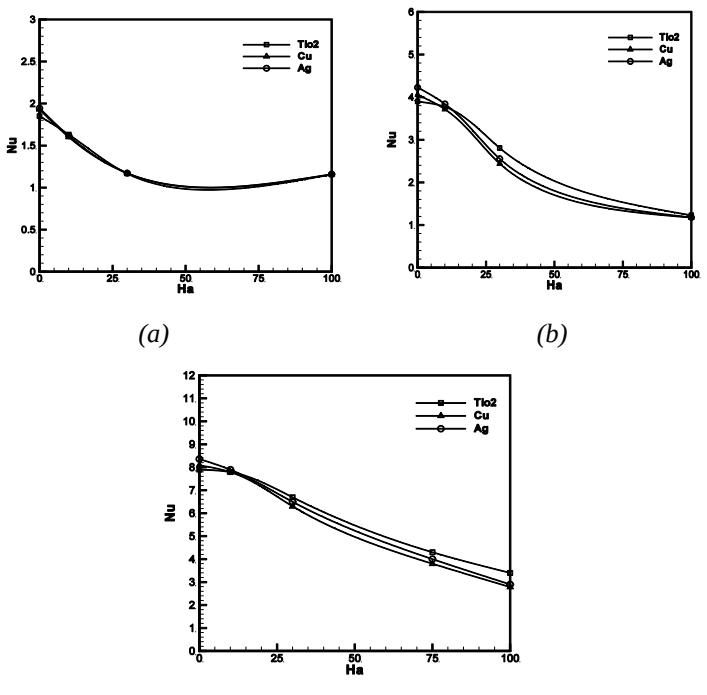

Figure 9. Effect of Hartmann number on average Nusselt number for different type of nano particles used at operating Rayleigh numbers (a) Ra=1.0e4 (b) Ra=1.0e5 and (c) Ra=1.0e6

Figure 9 gives the comparison of Average Nusselt number with respect to increment in Ha value for different nano fluids with particle volume fraction 0.05.

Three different type of nano particles are chosen, in which Ag are having better thermal and electrical conductivity, $Ti0_2$ having the least. Figure 9a gives the results corresponding to Ra=1.0e4, here in this case the difference in heat transfer characteristics with addition of different nano particles is found minimum and Nusselt number is just above unity when value of Ha is greater than 25. At Ra=1.0e5, the difference in Nusselt number is seen better with change in type of nano particles, Ag-nano fluid has exhibited higher heat transfer characteristics and TiO_2 has shown least at Ha=0. With increase in Hartmann number the difference between these three nano fluids is observed better because of difference in hampering effect experienced by each. TiO_2nano fluid is least influenced by magnetic field due to its low electrical conductivity.

Thus higher Nusselt number is recorded in the case of TiO_2nano fluid. Both Cu and Ag nano fluids have shown more or less similar characteristics with increase in magnetic field intensity. At Ha=100 again the value of Nu has reached close to unity and the difference in heat transfer experienced has decreased as a result of strong hampering. In case of Ra=1.0e6 such phenomenon has not occurred, even at Ha=100 the fluid convection is not completely hampered and TiO_2 case continues to dominate.

Figure 10 gives the comparison of average Sherwood number of different nano fluids with respect of change in magnetic field. At Ha=0 slight difference is observed in mass transfer rate among different particles, addition of TiO_2 particles which are relativity lighter reported in better mass transfer rates compared to others. As similar to heat transfer in case of mass transfer also the suppressing effect on mass transfer is found relatively minimum when TiO_2 nano particles are used. Among Cu and Ag nano particles, addition of Ag nano particles has resulted in slightly more loss in Sherwood number which may be because of its better polarization characteristics, higher density. Similar to Nusselt number the differences in mass transfer rates with application of magnetic field is not clearly seen at low Rayleigh number where the mass transfer rates experienced are already low and the transport process is mostly through diffusion mode for Ha>25.

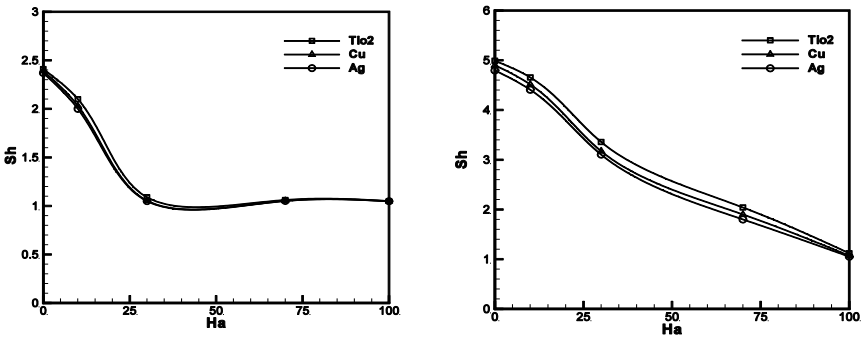

(a) *(b)*

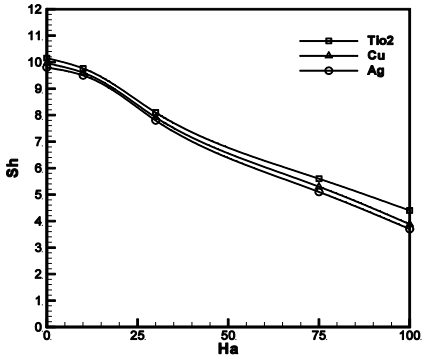

(c)

Figure 10. Effect of Hartmann number on average Sherwood number for different type of nano particles used at operating Rayleigh numbers (a) Ra=1.0e4 (b) Ra=1.0e5 and (c) Ra=1.0e6

5. Conclusion

Numerical investigations are carried out on the double diffusive convection flow of nano fluids in a square cavity under the influence of magnetic field. Various experiments are carried out on the effect of change in particle volume fraction and type of particles at various intensities of magnetic field and the thermal Rayleigh numbers using Galerkin's weighted residual finite element based code. Some of the important outcomes are reported below.

- Increase in Magnetic field intensity resulted in convection losses, at Ra=1.0e5 maximum of 71% and 78% loss is observed in Nusselt number and Sherwood number respectively with increment in Ha from 0 to 100.
- The relative increment in Nusselt number by addition of nano particles is observed slightly more when Ra=1.0e4 and relatively less at higher Rayleigh i.e Ra=1.0e6.
- Effectiveness of nanoparticles on Nu* enhancement is observed more when the magnetic field is on and any enchancement in magnetic field intensity showed positive effect.
- Similarly in case of relative mass transfer rates, the value of Sh* is found to decrease with inclusion of nano particles and increase in Ha from 0 to 100 has enhanced such phenomenon.
- Among different nano fluids, Ag-nano fluid has exhibited higher heat transfer characteristics and TiO_2 has shown least when no magnetic field is acting.
- But higher Nusselt number is recorded in this case of $Ti0_2$ nano fluid when magnetic field is enforced. Both Cu and Ag nano fluids have shown more or less

similar characteristics with increase in magnetic field intensity.

– The differences in both heat and mass transfer rates between different fluids with application of magnetic field is seen well when the magnetic intensity is low.

Reference

Abu-Nada E., Oztop H. (2009). Effects of inclination angle on natural convection in enclosures filled with Cu-water nanofluid. *International Journal of Heat and Fluid Flow*, Vol. 30, No. 4, pp. 669-678. http://doi.org/10.1016/j.ijheatfluidflow.2009.02.001

Akbarinia A., Behzadmehr A. (2007). Numerical study of laminar mixed convection of a nanofluid in horizontal curved tubes. *Applied Thermal Engineering*, Vol. 27, No. 8-9, pp. 1327-1337. http://doi.org/10.1016/j.applthermaleng.2006.10.034.

Al-Amiri A. M., Khanafar K. M., Pop I. (2007). Numerical simulation of a combined thermal mass transport in a square lid-driven cavity. *International Journal of Thermal Sciences*, Vol. 46, No. 7, pp. 662-671. http://doi.org/10.1016/j.ijthermalsci.2006.10.003

Alchaar S., Vasseur P., Bilgen E. (2007). Natural convection heat transfer in a rectangular enclosure with a transverse magnetic field. *ASME Journal of Heat Transfer*, Vol. 117, No. 3, pp. 668-673. http://doi.org/10.1115/1.2822628

Ashorynejad H. R., Mohamad A. A., Sheikholeslami M. (2013). Magnetic field effects on natural convection flow of a nanofluid in a horizontal cylindrical annulus using Lattice Boltzmann Method. *International Journal of Thermal Sciences*, Vol. 64, pp. 240–250. http://doi.org/10.1016/j.ijthermalsci.2012.08.006

Beghein C., Haghighat F., Allard F. (1992). Numerical study of double-diffusive natural convection in a square cavity. *International Journal of Heat and Mass Transfer*, Vol. 35, No. 4, pp. 833–846. http://doi.org/10.1016/0017-9310(92)90251-M

Bourantas G., Loukopoulos V. (2014). MHD natural-convection flow in an inclined square enclosure filled with a micropolar-nanofluid. *International Journal of Heat and Mass Transfer*, Vol. 79, pp. 930–944. http://doi.org/10.1016/j.ijheatmasstransfer.2014.08.075

Brinkman H. C. (1952). The viscosity of concentrated suspensions and solution. *The Journal of Chemical Physics*, Vol. 20, No. 4, pp. 571-581. http://doi.org/ 10.1063/1.1700493

Chamkha A. J., Al-Naser H. (2002). Hydromagnetic double-diffusive convection in a rectangular enclosure with uniform side heat mass fluxes opposing temperature concentration gradients. *International Journal of Thermal Sciences*, Vol. 41, pp. 936-948. http://doi.org/10.1016/S1290-0729(02)01386-8

Chamkha A. J., Al-Naser H. (2002). Hydromagnetic double-diffusive convection in a rectangular enclosure with opposing temperature concentration gradients. *International Journal of Heat and Mass Transfer*, Vol. 45, pp. 2465–2483. http://doi.org/10.1016/S0017-9310(01)00344-1

Chaves C. A., Lamas W. Q., Nunes L., Camargo J. R., Grandinetti F. J. (2015). Notes on steady natural convection heat transfer by double diffusion from a heated cylinder buried in a saturated porous media. *ASME Journal of Heat Transfer*, Vol. 137, No. 7, pp. 074501-074508. http://doi.org/10.1115/1.4029878

Chen S., Tolke J., Krafczyk M. (2010). Numerical investigation of double-diffusive (natural) convection in vertical annuluses with opposing temperature concentration gradients. *International Journal of Heat and Fluid Flow*, Vol. 31, pp. 217–226. http://doi.org/10.1016/j.ijheatfluidflow.2009.12.013

Corcione M., Grignaffini S., Quintino A. (2015). Correlations for the double-diffusive natural convection in square enclosures induced by opposite temperature concentration gradients. *International Journal of Heat and Mass Transfer*, Vol. 81, pp. 811–819. http://doi.org/10.1016/j.ijheatmasstransfer.2014.11.013

Drew D. A., Passman S. L. (1999). Theory of MulticomponentFluids, *Springer*, http://doi.org/101007/b97678

Emery A. F. (1963). The effect of a magnetic field upon the free convection of a conducting fluid. *ASME Journal of Heat Transfer*, Vol. 85, No. 2, pp. 119-124. http://doi.org/10.1115/1.3686025

Ghasemi B., Aminossadati S. M., Raisi A. (2011). Magnetic field effect on natural convection in a nanofluid-filled square enclosure. *International Journal of Thermal Sciences*, Vol. 50, pp. 1748–1756. http://doi.org/10.1016/j.ijthermalsci.2011.04.010

Ghernaout B., Bouabdallah S., Benchatti A., Bessaih R. (2014). Effect of the buoyancy ratio on oscillatory double-diffusive convection in binary mixture. *Numerical Heat Transfer Part A: Applications*, Vol. 66, No. 8, pp. 928-946. http://doi.org/10.1080/10407782.2014.892386

Jenaa S. K., Mahapatra S. K., Sarkar A., Chamkhac A. J. (2015). Thermo-solutal buoyancy-opposed free convection of a binary Ostwald–De Waele fluid inside a cavity having partially-active vertical walls. *Journal of the Taiwan Institute of Chemical Engineers*, Vol. 51, pp. 9–19. http://doi.org/10.1016/j.jtice.2015.01.007

Kefayati G. H. R. (2013). Effect of a magnetic source on natural convection in an open cavity subjugated to water/alumina nanofluid using Lattice Boltzmann Method. *International Journal of Heat and Mass Transfer*, Vol. 40, pp. 67–77. http://doi.org/10.1016/j.icheatmasstransfer.2012.10.024

Kefayati G. H. R. (2016). Simulation of heat transfer and entropy generation of MHD natural convection of non-Newtonian nanofluid in an enclosure. *International Journal of Heat and Mass Transfer*, Vol. 92, pp. 1066–1089. http://doi.org/10.1016/j.ijheatmasstransfer.2015.09.078

Kumar D. S., Murugesan K., Gupta A. (2010). Numerical analysis of interaction between inertial and thermosolutal buoyancy forces on convective heat transfer in a lid-driven cavity. *Journal of Heat Transfer*, Vol. 132, No. 11, pp. 112501. http://doi.org/10.1115/1.4002029

Kumar D. S., Murugesan K., Thomas H. R. (2011). Effect of the aspect ratio of a heated block on the interaction between inertial thermosolutal buoyancy forces in a lid- driven cavity. *Numerical Heat Transfer, Part A: Applications*, Vol. 60, No. 7, pp. 604-628. http://doi.org/10.1080/10407782.2011.609094

Lee J. W., Hyun J. M. (1997). Double-diffusive convection in a rectangle with opposing horizontal temperature and concentration gradients. *International Journal of Heat and Mass Transfer*, Vol. 33, pp. 1619–1632. http://doi.org/10.1016/0017-9310(90)90018-p

Ma C. (2009). Lattice BGK simulations of double diffusive natural convection in a rectangular enclosure in the presences of magnetic field heat source. *Nonlinear Anal Real World*, Vol. 10, pp. 2666-2678. http://doi.org/10.1016/j.nonrwa.2008.07.006

Mahapatra T. R., Pal D., Mondal S. (2013). Effects of buoyancy ratio on double-diffusive natural convection in a lid-driven cavity. *International Journal of Heat and Mass Transfer*, Vol. 57, pp.771–785. http://doi.org/10.1016/j.ijheatmasstransfer.2012.10.028

Mahmoudi A., Mejri I., Abbassi M. A., Omri A. (2015). Analysis of MHD natural convection in a nanofluid-filled open cavity with non-uniform boundary condition in the presence of uniform heat generation/absorption. *Powder Technology*, Vol. 269, pp. 275–289. http://doi.org/10.1016/j.powtec.2014.09.022

Mahmoudi A., Mejri I., Abbassi M. A., Omri A. (2014). Analysis of the entropy generation in a nanofluid-filled cavity in the presence of magnetic field and uniform heat generation/absorption. *Journal of Molecular Liquids*, Vol. 198, pp. 63–77. http://doi.org/10.1016/j.molliq.2014.07.010

Maiga S. E. B., Palm S. J., Nguyen C. T., Roy G., Galanis N. (2005). Heat transfer enhancement by using nanofluids in forced convection flows. *International Journal of Heat and Fluid Flow*, Vol. 26, No. 4, pp. 530-546. http://doi.org/10.1016/j.ijheatfluidflow.2005.02.004

Motevasel M., Nazar A. R. S., Jamialahmadi M. (2017). Experimental investigation of turbulent flow convection heat transfer of MgO/water nanofluid at low concentrations–Prediction of aggregation effect of nanoparticles. *International Journal of Heat and Technology*, Vol. 35, No. 4, pp. 755-764. http://doi.org/10.18280/ijht.350409

Nazari M., Louhghalam L., Kayhani M. H. (2015). Lattice Boltzmann simulation of double diffusive natural convection in a square cavity with a hot square obstacle. *Chinese Journal of Chemical Engineering*, Vol. 23, pp. 22–30. http://doi.org/10.1016/j.cjche.2014.10.008

Nishimura T., Wakamatsu M., Morega A. M. (1998). Oscillatory double diffusive convection in a rectangular enclosure with combined horizontal temperature concentration gradients. *International Journal of Heat and Mass Transfer*, Vol. 41, pp. 1601-1611. http://doi.org/10.1016/S0017-9310(97)00271-8

Qin Q., Za, X., Tian Z. F. (2014). High accuracy numerical investigation of double-diffusive convection in a rectangular enclosure with horizontal temperature concentration Gradients. *International Journal of Heat and Mass Transfer*, Vol. 71, pp. 405–423. http://doi.org/10.1016/j.ijheatmasstransfer.2013.12.035

Reddy N., Murugesan K. (2017). Numerical investigations on the advantage of nano fluids under DDMC in a lid driven cavity, Wiley. *Heat transfer- Asian Research*, Vol. 46, No. 7, pp. 1065-1086. http://doi.org/10.1002/htj.21260

Reddy N., Murugesan K. (2017). Magnetic field influence on double diffusive natural convection in a square cavity-A numerical study. *Taylor and Fransis, Numerical Heat Transfer*, Vol. 71, No. 4, pp. 448-475. http://doi.org/10.1080/10407782.2016.1277922

Reddy N., Murugesan K. (2017). Numerical study of double diffusive convection in a lid driven cavity with linearly salted side walls. *Journal of Applied Fluid mechanics*, Vol. 10, No. 1, pp. 69-79. http://doi.org/10.18869/acadpub.jafm.73.238.26231

Ren Q., Chan C. L. (2016). Numerical study of double-diffusive convection in a vertical cavity with Soret Dufour effects by lattice Boltzmann method on GPU. *International Journal of Heat and Mass Transfer*, Vol. 93, pp. 538-553. http://doi.org/10.1016/j.ijheatmasstransfer.2015.10.031

Seki M., Kawamura H., and Sanokawa K. (1979). Natural convection of mercury in a magnetic field parallel to the gravity. *ASME Journal of Heat Transfer*, Vol. 101, No. 2, pp. 227-232. https://doi.org/10.1115/1.3450951

Selimefendigil F., Oztop H. F. (2014). Numerical study of MHD mixed convection in a nanofluid filled lid driven square enclosure with a rotating cylinder. *International Journal of Heat and Mass Transfer*, Vol. 78, pp. 741–754. http://doi.org/10.1016/j.ijheatmasstransfer.2014.07.031

Sheikholeslami M., Gorji-Bandpy M., Ganji D. D. (2014). Lattice Boltzmann method for MHD natural convection heat transfer using nanofluid. *Powder Technology*, Vol. 254, pp. 82-93. http://doi.org/10.1016/j.powtec.2013.12.054

Siddiqa S., Hossain M. A., Saha S. C. (2012). Double diffusive magneto-convection fluid flow in a strong cross magnetic field with uniform surface heat mass flux. *ASME Journal of Heat Transfer*, Vol. 134, No. 11, pp.114506-1. http://doi.org/10.1115/1.4007130

Singh P., Kumar M. (2015). Mass transfer in MHD flow of alumina water nanofluid over a flat plate under slip conditions. *Alexandria Engineering Journal*, Vol. 54, pp. 383-387. http://doi.org/10.1016/j.aej.2015.04.005

Sourtiji E., Gorji-Bandpy M., Ganji D. D., Seyyedi S. M. (2014). Magnetohydrodynamic buoyancy-driven heat transfer in a cylindrical–triangular annulus filled by Cu– water nanofluid using CVFEM. *Journal of Molecular Liquids*, Vol. 196, pp. 370–380. http://doi.org/10.1016/j.molliq.2014.04.017

Teamah M. A. (2008). Numerical simulation of double diffusive natural convection in rectangular enclosure in the presences of magnetic field heat source. *International Journal of Thermal Sciences*, Vol. 47, pp. 237-248. http://doi.org/10.1016/j.ijthermalsci.2007.02.003

Vasanthakumari R., Pondy P. (2018). Mixed convection of silver and titanium dioxide nanofluids along inclined stretching sheet in presence of MHD with heat generation and suction effect. *Mathematical Modelling of Engineering Problems*, Vol. 5, No. 2, pp. 123-129. http://doi.org/10.18280/mmep.050210

Venkatachalapa M., Younghae D., Sankar M. (2011). Effect of magnetic field on the heat mass transfer in a vertical annulus. *International Journal of Engineering Science*, Vol. 49, No. 3, pp. 262-278. http://doi.org/10.1016/j.ijengsci.2010.12.002

Xu B., Li B. Q., Stock D. E. (2006). An experimental study of thermally induced convection of molten gallium in magnetic fields. *International Journal of Heat and Mass Transfer*, Vol. 49, pp. 2009–2019. http://doi.org/10.1016/j.ijheatmasstransfer.2005.11.033

Nomenclature

AR	aspect ratio
C	concentration of species, kg/m^3
D	binary diffusion coefficient, m^2/s
G	gravitational acceleration, $m.s^{-2}$
Gr	Grash of number
H	height of the cavity
Ha	Hartmann number

Le	Lewis number
N	buoyancy ratio
Nu	local Nusselt number
Nu*	effective Nusselt number
Pr	Prandtl number
Re	Reynolds number
Ri	Rayleigh number
Sc	Schmidt number
Sh	local Sherwood number
t	time, s
T	temperature, K
u,v	horizontal and vertical velocity components, m/s
U, V	non-dimensional velocity components
U0	lid velocity, m
VF	volume fraction of nano particles
x, y	horizontal and vertical coordinates, m
X, Y	non dimensional coordinates

Greek symbol

α	thermal diffusivity, $m^2.\ s^{-1}$
βC	concentration volumetric expansion coefficient, m^3/kg
βT	thermal volumetric expansion coefficient, K-
μ	dynamic viscosity, kg. $m^{-1}.s^{-11}$
υ	kinematic viscosity, m^2/s
ϕ	non dimensional concentration of species
Θ	non-dimensional temperature
ρ	density, kg/m^3
τ	non dimensional time
ω	vorticity, s^{-1}
ς	non dimensional vorticity

Subscripts

Av	average
C	cold
H	hot
Nf	nano fluid
F	base fluid
p	particle